Experimental Separation of Rashba and Dresselhaus Spin Splittings in Semiconductor Quantum Wells

S. D. Ganichev,[1,2] V.V. Bel'kov,[2] L. E. Golub,[2] E. L. Ivchenko,[2] Petra Schneider,[1] S. Giglberger,[1] J. Eroms,[1] J. De Boeck,[3] G. Borghs,[3] W. Wegscheider,[1] D. Weiss,[1] and W. Prettl[1]

[1]*Fakultät Physik, University of Regensburg, 93040, Regensburg, Germany*
[2]*A. F. Ioffe Physico-Technical Institute, Russian Academy of Sciences, 194021 St. Petersburg, Russia*
[3]*IMEC, Kapeldreef 75, B-3001 Leuven, Belgium*

(Received 2 June 2003; published 23 June 2004)

The relative strengths of Rashba and Dresselhaus terms describing the spin-orbit coupling in semiconductor quantum well (QW) structures are extracted from photocurrent measurements on *n*-type InAs QWs containing a two-dimensional electron gas (2DEG). This novel technique makes use of the angular distribution of the spin-galvanic effect at certain directions of spin orientation in the plane of a QW. The ratio of the relevant Rashba and Dresselhaus coefficients can be deduced directly from experiment and does not relay on theoretically obtained quantities. Thus our experiments open a new way to determine the different contributions to spin-orbit coupling.

DOI: 10.1103/PhysRevLett.92.256601 PACS numbers: 72.25.Fe, 73.21.Fg, 73.63.Hs, 78.67.De

The manipulation of the spin of charge carriers in semiconductors is one of the key problems in the field of spintronics (see, e.g., [1]). In the paradigmatic spin transistor, e.g., proposed by Datta and Das [2], the electron spins, injected from a ferromagnetic contact into a two-dimensional electron system are controllably rotated during their passage from source to drain by means of the Rashba spin-orbit coupling [3]. The coefficient α, which describes the strength of the Rashba spin-orbit coupling, and hence the degree of rotation, can be tuned by gate voltages. This coupling stems from the inversion asymmetry of the confining potential of two-dimensional electron (or hole) systems. The dependence of α on the gate voltage has been shown experimentally by analyzing the beating pattern observed in Shubnikov–de Haas (SdH) oscillations [4–10]. In addition to the Rashba coupling, caused by structure inversion asymmetry (SIA), also a Dresselhaus type of coupling contributes to the spin-orbit interaction. The latter is due to bulk inversion asymmetry (BIA) [11,12] and the interface inversion asymmetry (IIA) [13,14]. The BIA and IIA contributions are phenomenologically inseparable and described below by the generalized Dresselhaus parameter β. Both Rashba and Dresselhaus couplings result in spin splitting of the band (Fig. 1) and give rise to a variety of spin dependent phenomena that allow one to evaluate the magnitude of the total spin splitting of electron subbands.

However, usually it is not possible to extract the relative contributions of Rashba and Dresselhaus terms to the spin-orbit coupling. To obtain the Rashba coefficient α, the Dresselhaus contribution is normally neglected [5–10]. At the same time, Dresselhaus and Rashba terms can interfere in such a way that macroscopic effects vanish though the individual terms are large [15,16]. For example, both terms can cancel each other, resulting in a vanishing spin splitting in certain $\boldsymbol{k}$-space directions [17]. This cancellation leads to the disappearance of an antilocalization [18], the absence of spin relaxation in specific crystallographic directions [15,19], and the lack of SdH beating [16]. In a recent paper [20] the importance of both Rashba and Dresselhaus terms was pointed out: tuning α such that $\alpha = \beta$ holds, allows one to build a nonballistic spin-field effect transistor.

Below we demonstrate that angular dependent measurements of the spin-galvanic photocurrent [21,22]

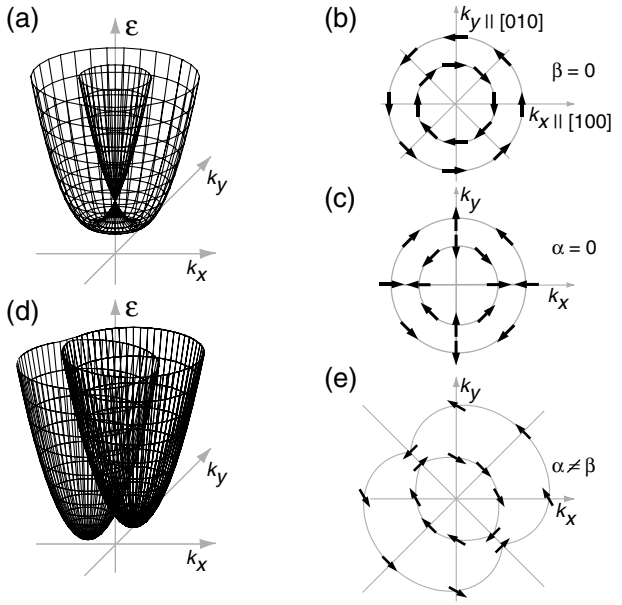

FIG. 1. Schematic 2D band structure with $\boldsymbol{k}$-linear terms for C_{2v} symmetry for different relative strengths of SIA and BIA and the distribution of spin orientations at the 2D Fermi energy: (a) The case of only Rashba or Dresselhaus spin-orbit coupling. (d) The case of the simultaneous presence of both contributions. Arrows indicate the orientation of spins.

allow one to separate contributions due to Dresselhaus and Rashba terms. Here, we make use of the fact that these terms contribute differently for particular crystallographic directions. Hence, by mapping the magnitude of the photocurrent in the plane of the quantum well (QW) the ratio of both terms can be directly determined from experiment.

Before turning to experiment we briefly summarize the consequences of Rashba and Dresselhaus terms on the electron dispersion and on the spin orientation of the electronic states of the two-dimensional electron gas (2DEG). We consider QWs of the zinc-blende structure grown in the [001] direction. For the corresponding C_{2v} symmetry the spin-orbit part $\hat{H}_{SO}$ of the Hamiltonian $\hat{H} = \hbar^2 \boldsymbol{k}^2/2m^* + \hat{H}_{SO}$ contains the Rashba term as well as the Dresselhaus term according to

$$\hat{H}_{SO} = \alpha(\sigma_x k_y - \sigma_y k_x) + \beta(\sigma_x k_x - \sigma_y k_y), \quad (1)$$

where $\boldsymbol{k}$ is the electron wave vector, and $\boldsymbol{\sigma}$ is the vector of the Pauli matrices. Here, the x axis is aligned along the [100] direction, y is aligned along [010], and z is the growth direction (see Fig. 1). The Hamiltonian of Eq. (1) contains only terms linear in $\boldsymbol{k}$. As we show below, terms cubic in $\boldsymbol{k}$ in our experiments change only the strength of β leaving the Hamiltonian unchanged.

To illustrate the resulting energy dispersion in Fig. 1 we plot the eigenvalues of $\hat{H}$, $\varepsilon(\boldsymbol{k})$, and contours of constant energy in the k_x,k_y plane for different ratios of α and β. For $\alpha \neq 0, \beta = 0$ and $\alpha = 0, \beta \neq 0$ the dispersion has the same shape and consists of two shifted parabolas in all directions, displayed in Fig. 1(a). However, Rashba and Dresselhaus terms result in a different pattern of the eigenstate's spin orientation in $\boldsymbol{k}$ space. The distribution of this spin orientation can be visualized by writing the spin-orbit interaction term in the form $\hat{H}_{SO} = \boldsymbol{\sigma} \cdot \boldsymbol{B}_{eff}(\boldsymbol{k})$ where $\boldsymbol{B}_{eff}(\boldsymbol{k})$ is an effective magnetic field that provides the relevant quantization axes [23]. By comparison with Eq. (1) one obtains for pure Rashba ($\beta = 0$) and pure Dresselhaus ($\alpha = 0$) coupling the corresponding effective magnetic fields, $\boldsymbol{B}_{eff}^{(R)} = \alpha(k_y, -k_x)$ and $\boldsymbol{B}_{eff}^{(D)} = \beta(k_x, -k_y)$, respectively. The spin orientations for Rashba and Dresselhaus coupling are schematically shown in Figs. 1(b) and 1(c) by arrows. Here it is assumed that $\alpha > \beta > 0$. For the Rashba case the effective magnetic field, and hence the spin, is always perpendicular to the corresponding $\boldsymbol{k}$ vector [Fig. 1(b)]. In contrast, for the Dresselhaus contribution, the angle between the $\boldsymbol{k}$ vector and spin depends on the direction of $\boldsymbol{k}$. In the presence of both Rashba and Dresselhaus spin-orbit couplings, relevant for C_{2v} symmetry, the $[1\bar{1}0]$ and the [110] axes become strongly nonequivalent. For $\boldsymbol{k} \parallel [1\bar{1}0]$ the eigenvalues of the Hamiltonian are then given by $\varepsilon = \hbar^2 \boldsymbol{k}^2/2m^* \pm (\alpha - \beta)|\boldsymbol{k}|$ and for $\boldsymbol{k} \parallel [110]$ by $\varepsilon = \hbar^2 \boldsymbol{k}^2/2m^* \pm (\alpha + \beta)|\boldsymbol{k}|$. This anisotropic dispersion $\varepsilon(\boldsymbol{k})$ is sketched in Fig. 1(d), and the corresponding contours of constant energy together with the spin orientation of selected $\boldsymbol{k}$ vectors are shown in Fig. 1(e).

Angular dependent investigations of spin photocurrents provide a direct measure of the anisotropic orientation of spins in $\boldsymbol{k}$ space and hence of the different contributions of the Rashba and the Dresselhaus terms. We employ the spin-galvanic effect to extract the ratio of the Rashba and the Dresselhaus contributions. The spin-galvanic current is driven by the electron in-plane average spin $\boldsymbol{S}_\parallel$ according to [17,21]

$$\boldsymbol{j}_{SGE} \propto \begin{pmatrix} \beta & -\alpha \\ \alpha & -\beta \end{pmatrix} \boldsymbol{S}_\parallel. \quad (2)$$

Therefore, the spin-galvanic current $\boldsymbol{j}_{SGE}$ for a certain direction of $\boldsymbol{S}_\parallel$ consists of Rashba and Dresselhaus coupling induced currents, $\boldsymbol{j}_R$ and $\boldsymbol{j}_D$ [see Fig. 2(a)]. Their magnitudes are $j_R \propto \alpha|\boldsymbol{S}_\parallel|$ and $j_D \propto \beta|\boldsymbol{S}_\parallel|$, and their ratio is

$$j_R/j_D = \alpha/\beta. \quad (3)$$

For $\boldsymbol{S}_\parallel$ oriented along one of the cubic axes it follows from Eq. (2) that the currents flowing along and perpendicular to $\boldsymbol{S}_\parallel$ are equal to j_D and j_R, respectively, yielding experimental access to determine α/β.

The experiments are carried out on (001)-oriented n-type heterostructures having C_{2v} point symmetry. $InAs/Al_{0.3}Ga_{0.7}Sb$ single QW of 15 nm width with free carrier densities of about 1.3×10^{12} cm^{-2} and mobility at room temperature $\approx 2 \times 10^4$ cm^2/(V s) were grown by molecular-beam epitaxy. Several samples of the same batch were investigated at room temperature yielding the same results. The sample edges are oriented along the $[1\bar{1}0]$ and [110] crystallographic axes. Eight pairs of contacts on each sample allow one to probe the photocurrent in different directions [see Fig. 2(b)]. For optical spin orientation we use a high power pulsed molecular far-infrared NH_3 laser [24]. The linearly polarized radiation at a wavelength 148 μm with a power of 10 kW is modified to be circularly polarized by using a $\lambda/4$ quartz plate. The photocurrent $\boldsymbol{j}_{SGE}$ is measured in unbiased structures via the voltage drop across a 50 Ω load resistor in a closed circuit configuration [17]. It is detected for right (σ_+) and left (σ_-) handed circularly polarized radiation. The spin-galvanic current j_{SGE}, studied here, is extracted after eliminating current contributions that

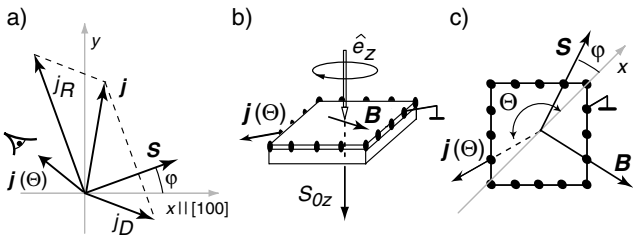

FIG. 2. Angular dependence of the spin-galvanic current (a) and the geometry of the experiment (b),(c).

are helicity independent [25]: $j_{\mathrm{SGE}} = (j_{\sigma_+} - j_{\sigma_-})/2$. Note that the spin-galvanic current is of the same order as the background current (see [25]).

The nonequilibrium in-plane spin polarization $\boldsymbol{S}_\parallel$ is prepared as described recently [21]: Circularly polarized light at normal incidence on the 2DEG plane, induces indirect (Drude-like) electron transitions in the lowest conduction subband of our n-type samples resulting in a monopolar spin orientation [26] in the z direction [Fig. 2(b)]. An in-plane magnetic field ($B = 1$ T) rotates the spin around the magnetic field axis (precession) and results in a nonequilibrium in-plane spin polarization $S_\parallel \propto \omega_L \tau_s$, where ω_L is the Larmor frequency and τ_s is the spin-relaxation time. In the range of the applied magnetic field strength the spin-galvanic current in the present samples at room temperature rises linearly with B indicating $\omega_L \tau_s < 1$ and, thus, the Hanle effect is not present (see [25]). The angle between the magnetic field and $\boldsymbol{S}_\parallel$ in general depends on details of the spin-relaxation process. In the InAs QW structure investigated here, the isotropic Elliot-Yafet spin-relaxation mechanism dominates [15,27]. Thus the in-plane spin polarization $\boldsymbol{S}_\parallel$ of photoexcited carriers is always perpendicular to $\boldsymbol{B}$ and can be varied by rotating $\boldsymbol{B}$ around z as illustrated in Fig. 2(c). This excess spin polarization $\boldsymbol{S}_\parallel$ leads to an increase of the population of the corresponding spin-polarized states. Because of asymmetric spin relaxation an electric current results [21].

To obtain the Rashba and Dresselhaus contributions the spin-galvanic effect is measured for a fixed orientation of $\boldsymbol{S}_\parallel$ for all accessible directions Θ [see Fig. 2(c)]. According to Eq. (2) the current $\boldsymbol{j}_R$ always flows perpendicularly to the spin polarization $\boldsymbol{S}_\parallel$, and $\boldsymbol{j}_D$ encloses an angle -2φ with $\boldsymbol{S}_\parallel$. Here φ is the angle between $\boldsymbol{S}_\parallel$ and the x axis. Then, the current component along any direction given by angle Θ can be written as a sum of the projections of $\boldsymbol{j}_R$ and $\boldsymbol{j}_D$ on this direction

$$j_{\mathrm{SGE}}(\Theta) = j_D \cos(\Theta + \varphi) + j_R \sin(\Theta - \varphi). \qquad (4)$$

Three directions of spin population $\boldsymbol{S}_\parallel$ are particularly suited to extract the ratio between Rashba and Dresselhaus terms. These geometries are sketched in Figs. 3(a)–3(c), left column. In Fig. 3(a), the spin polari-zation $\boldsymbol{S}_\parallel$ is set along [100] ($\varphi = 0$). Then from Eq. (4) follows that the currents along the [100] direction ($\Theta = 0$) and the [010] direction ($\Theta = \pi/2$) are equal to j_D and j_R, respectively, as shown on the left hand side of Fig. 3(a). Figure 3(b) illustrates another geometry. For a nonequilibrium spin polarization induced along [110] ($\varphi = \pi/4$) Eq. (4) predicts that the current has its maximum value $j = j_R - j_D$ at $\Theta = 3\pi/4$. If the spin is aligned along $[1\bar{1}0]$ [$\varphi = -\pi/4$ in Fig. 3(c)], on the other hand, the maximum current $j = j_R + j_D$ is expected to flow under an angle of $\Theta = \pi/4$. Thus, the relative strength of the measured $j_R - j_D$ and $j_R + j_D$ values allows a straightforward determination of $j_R/j_D = \alpha/\beta$.

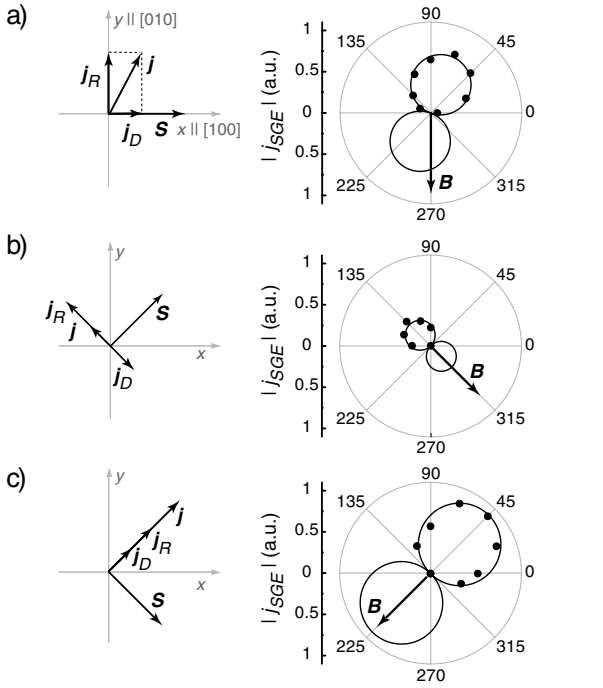

FIG. 3. Photocurrent in n-type InAs single QWs. Left plates indicate three selected relations between spin polarization and current contributions [after Eq. (2)]. Right plates show measurements of the spin galvanic current as a function of angle Θ. Data are presented in polar coordinates. The magnitude of the current measured at the radiation power of 10 kW is normalized to the current maximum ($j_{\max} = 20\ \mu$A) obtained in the geometry of (c).

The results are shown in Fig. 3. The left hand side of Fig. 3 displays the geometric arrangement discussed above and shows the direction of the photogenerated spins $\boldsymbol{S}_\parallel$ and the resulting Rashba and Dresselhaus currents. The corresponding experimentally obtained currents measured in different directions are presented in polar coordinates on the right hand side of the figure. The current's magnitude is normalized to the maximum value of the spin-galvanic current obtained if Rashba and Dresselhaus contributions point in the same direction [Fig. 3(c)]. The ratio of Rashba and Dresselhaus currents can be directly read off from the right hand side of Fig. 3(a), $j_R/j_D = j(\pi/2)/j(0)$, or can be evaluated from the maximum currents j in Figs. 3(b) and 3(c). Both procedures give the same result: $j_R/j_D = 2.15 \pm 0.25$. Moreover, all data on the right hand side of Fig. 3 are in excellent agreement with the picture given above: Using $\alpha/\beta = 2.15$, the three sets of the data points can be fitted simultaneously by Eq. (4) without additional fitting parameters.

The value of 2.15 agrees with theoretical results [28], which predict a dominating Rashba spin-orbit coupling for InAs QWs and is also consistent with recent experiments [6,18]. For InGaAs QWs, having similar sample parameters as the devices investigated here, α/β ratios were obtained from weak antilocalization experiments

[18] and $\boldsymbol{k} \cdot \boldsymbol{p}$ calculations [29]. The corresponding values ranged between 1.5–1.7 and 1.85, respectively. These results are in good agreement with our findings. The ratio of Rashba and Dresselhaus terms has previously been estimated by means of Raman spectroscopy [30] and transport investigations [18,31]. In contrast to these works our method allows one to measure directly the relative strength of Rashba and Dresselhaus terms and does not require any additional theoretical estimations.

So far we have not addressed the role of a contribution cubic in $\boldsymbol{k}$ in the Hamiltonian $\hat{H}_{\mathrm{SO}}$. This results in terms proportional to k^3 in the Hamiltonian, which vary with the angle $\vartheta_{\boldsymbol{k}}$ between $\boldsymbol{k}$ and the x axis. The angle appears as a linear combination of first and third order harmonics, i.e., as combinations of $\cos\vartheta_{\boldsymbol{k}}$, $\sin\vartheta_{\boldsymbol{k}}$ and $\cos 3\vartheta_{\boldsymbol{k}}$, $\sin 3\vartheta_{\boldsymbol{k}}$ terms (see, for instance, [18,32]). The spin-galvanic effect, on the other hand, is related to only the first order harmonics in the Fourier expansion of the nonequilibrium electron distribution function [32]. Hence, a cubic contribution leaves—for our photocurrent measurements—the form of the Hamiltonian unchanged (though it modifies the spin splitting [30–33]) but renormalizes only the Dresselhaus constant β: The coefficient $\beta = \gamma\langle k_z^2\rangle$ describing $\boldsymbol{k}$-linear terms should be replaced by $\beta = \gamma(\langle k_z^2\rangle - k^2/4)$. Here γ is the bulk spin-orbit constant and $\langle k_z^2\rangle$ is the averaged squared wave vector in the growth direction (see, for instance, [18,32]).

In conclusion, we have shown that photocurrent measurements provide a new way to extract direct information on the different contributions to spin-orbit coupling. We note that also the circular photogalvanic effect [34] can be used to separate Rashba and Dresselhaus contributions. The same qualitative result for the ratio α/β was obtained [35]. In contrast to the spin-galvanic effect applied here, where a small in-plane magnetic field to prepare the necessary in-plane spin orientation $\boldsymbol{S}_{\parallel}$ is used, the circular photogalvanic effect does not require an external magnetic field. The method can also be used for other material systems like GaAs quantum wells, where, instead of the isotropic Elliot-Yafet spin-relaxation mechanism, the anisotropic D'yakonov-Perel mechanism dominates. In this case the anisotropy of the spin-relaxation process [15], which results in an anisotropic spin distribution $\boldsymbol{S}_{\parallel}$, must be taken into account.

We thank T. Dietl for helpful discussion. This work is supported by the DFG, RFBR, INTAS, "Dynasty" Foundation—ICFPM, RAS, and Russian Ministries of Science and Education.

[1] *Semiconductor Spintronics and Quantum Computation*, edited by D. D. Awschalom, D. Loss, and N. Samarth (Springer, Berlin, 2002).
[2] S. Datta and B. Das, Appl. Phys. Lett. **56**, 665 (1990).
[3] Y. A. Bychkov and E. I. Rashba, Pis'ma Zh. Eksp. Teor. Fiz. **39**, 66 (1984) [Sov. Phys. JETP Lett. **39**, 78 (1984)].
[4] B. Das *et al.*, Phys. Rev. B **39**, 1411 (1989).
[5] J. Luo *et al.*, Phys. Rev. B **41**, 7685 (1990).
[6] J. Nitta *et al.*, Phys. Rev. Lett. **78**, 1335 (1997).
[7] G. Engels *et al.*, Phys. Rev. B **55**, R1958 (1997).
[8] J. P. Heida *et al.*, Phys. Rev. B **57**, 11 911 (1998).
[9] C. M. Hu *et al.*, Phys. Rev. B **60**, 7736 (1999).
[10] D. Grundler, Phys. Rev. Lett. **84**, 6074 (2000).
[11] M. I. D'yakonov and V. Yu. Kachorovskii, Fiz. Tekh. Poluprovodn. **20**, 178 (1986) [Sov. Phys. Semicond. **20**, 110 (1986)].
[12] U. Rössler *et al.*, in *High Magnetic Fields in Semiconductor Physics II*, edited by G. Landwehr, Springer Series in Solid State Sciences Vol. 87 (Springer-Verlag, Berlin, Heidelberg, 1989), p. 376.
[13] L. Vervoort and P. Voisin, Phys. Rev. B **56**, 12 744 (1997).
[14] U. Rössler and J. Kainz, Solid State Commun. **121**, 313 (2002).
[15] N. S. Averkiev *et al.*, J. Phys. Condens. Matter **14**, R271 (2002).
[16] S. A. Tarasenko and N. S. Averkiev, Pis'ma Zh. Eksp. Teor. Fiz. **75**, 669 (2002) [JETP Lett. **75**, 552 (2002)].
[17] S. D. Ganichev and W. Prettl, J. Phys. Condens. Matter **15**, R935 (2003), and references therein.
[18] W. Knap *et al.*, Phys. Rev. B **53**, 3912 (1996).
[19] N. S. Averkiev and L. E. Golub, Phys. Rev. B **60**, 15 582 (1999).
[20] J. Schliemann *et al.*, Phys. Rev. Lett. **90**, 146801 (2003).
[21] S. D. Ganichev *et al.*, Nature (London) **417**, 153 (2002).
[22] S. D. Ganichev *et al.*, Phys. Rev. B **68**, 081302 (2003).
[23] E. A. de Andrada e Silva, Phys. Rev. B **46**, 1921 (1992).
[24] S. D. Ganichev, Physica (Amsterdam) **273–274B**, 737 (1999).
[25] V. V. Bel'kov *et al.*, cond-mat/0311474.
[26] S. A. Tarasenko *et al.*, J. Supercond. **16**, 419 (2003).
[27] A. Takeuchi *et al.*, Physica (Amsterdam) **272B**, 318 (1999).
[28] G. Lommer *et al.*, Phys. Rev. Lett. **60**, 728 (1988).
[29] P. Pfeffer and W. Zawadzki, Phys. Rev. B **59**, R5312 (1999).
[30] B. Jusserand *et al.*, Phys. Rev. B **51**, 4707 (1995).
[31] J. B. Miller *et al.*, Phys. Rev. Lett. **90**, 076807 (2003).
[32] E. L. Ivchenko, and G. E. Pikus, *Superlattices and Other Heterostructures. Symmetry and Optical Phenomena* (Springer, Berlin, 1997).
[33] A. Łusakowski *et al.*, Phys. Rev. B **68**, 081201 (2003).
[34] S. D. Ganichev *et al.*, Phys. Rev. Lett. **86**, 4358 (2001).
[35] S. D. Ganichev *et al.* (unpublished).